Smart Structures and Systems, *Vol. 23, No. 6 (2019) 653-667*
DOI: https://doi.org/10.12989/sss.2019.23.6.653

Free vibrations of a two-cable network inter-supported by cross-links extended to ground

H.J. Zhou[1,2a], Y.H. Wu[1b], L.X. Li[*2], L.M. Sun[3c] and F. Xing[2d]

[1]*Institute of Urban Smart Transportation & Safety Maintenance, Shenzhen University, Nanhai Ave 3688, Shenzhen 518060, China*
[2]*Guangdong Provincial Key Laboratory of Durability for Marine Civil Engineering, Shenzhen University, Nanhai Ave 3688, Shenzhen, Guangdong 518060, P.R. China*
[3]*State Key Laboratory for Disaster Reduction in Civil Engineering, Tongji University, Siping Road1239, Shanghai 200092, P.R. China*

(Received July 2, 2016, Revised January 15, 2019, Accepted January 25, 2019)

Abstract. Using cross-ties to connect cables together when forming a cable network is regarded as an efficient method of mitigating cable vibrations. Cross-ties have been extended and fixed on bridge decks or towers in some engineering applications. However, the dynamics of this kind of system need to be further studied, and the effects of extending cross-links to bridge decks/towers on the modal response of the system should be assessed in detail. In this paper, a system of two cables connected by an inter-supported cross-link with another lower cross-link extended to the ground is proposed and analyzed. The characteristic equation of the system is derived, and some limiting solutions in closed form of the system are derived. Roots of cable system with special configurations are also discussed, attention being given to the case when the two cables are identical. A predictable mode behavior was found when the stiffness of inter-connection cross-link and the cross-link extended to the ground were the same. The vector of mode energy distribution and the degree of mode localization index are proposed so as to distinguish global and local modes. The change of mode behaviors is further discussed in the case when the two cables are not identical. Effects of cross-link stiffness, cross-link location, mass-tension ratio, cable length ratio and frequency ratio on 1st mode frequency and mode shape are addressed.

Keywords: cable network; cross-tie; vibration; frequency; mode shape

1. Introduction

Stay cables are crucial tension members when supporting the girders of cable-stayed bridges. However, stay cables are vulnerable to environmental excitation because of their slenderness and low damping characteristics (Virlogeux 1998, Kumarasena *et al.* 2007). A great deal of research literature is available describing wind, wind-rain and supporter-excited stay-cable vibration based upon field monitoring, analytical exploration and wind-tunnel simulations (Kumarasena *et al.* 2007, Zhou and Xu 2007, Xu *et al.* 2008). To suppress such kinds of harmful vibrations, different engineering solutions have been adopted, including cable surface modification (Kumarasena *et al.* 2007), the installation of near-support passive or semi-active dampers (Krenk 2000, Sun *et al*. 2004, Chen *et al.* 2004, Li *et al*. 2004, Bosch and Park 2005, Wang *et al.* 2005, Duan *et al.* 2005, 2006, 2019a, b, Christenson *et al.* 2006, Zhou *et al.* 2006, 2014b, Kumarasena *et al.* 2007, Zhou and Xu 2007, Fujino and Hoang 2008, Or *et al*. 2008, Zhou and Sun 2008 and 2013, Lu *et al*. 2017, Zhou *et al.* 2018a), the use of secondary cables (also known as cross-ties) (Kumarasena *et al.* 2007), and hybrid application of both cross-ties and dampers (Sun *et al.* 2005, Zhou *et al.* 2015, 2018b).

Connected cable system with cross-ties will increase the natural vibration frequencies of the system, which in turn increases the threshold critical wind speeds for triggering aerodynamic instabilities. Ehsan and Scanlan (1990) used component-mode synthesis and finite element approaches in the solution of a three-dimensional cable problem. Yamaguchi and Nagahawatta (1995) tested a two-cable network and used an energy method to evaluate the damping contribution of cross-ties. Virlogeux (1998) analyzed the field experience of the application of cross-ties in the Bridge of Normandie. Caracoglia and Jones (2005a) studied the linear dynamics of a two-cable network and further extended the analytical method to a prototype bridge cable network for the Fred Hartman Bridge. Sun *et al.* (2007) tested a three-cable networks model and evaluated the damping contribution from cross-ties. Giaccu and Caracoglia (2012) also studied the nonlinear effects of cross-ties, and a parametric study of a three-cable system with nonlinear restoring-force spring under stochastic free

*Corresponding author, Assistant Professor
E-mail: lilixiao@szu.edu.cn
[a] Professor
E-mail: haijun@szu.edu.cn
[b] Undergraduate Student
E-mail: 516920229@qq.com
[c] Professor
E-mail: lmsun@tongji.edu.cn
[d] Professor
E-mail: xingf@szu.edu.cn

http://www.techno-press.com/journals/sss&subpage=7
ISSN: 1738-1584 (Print), 1738-1991 (Online)

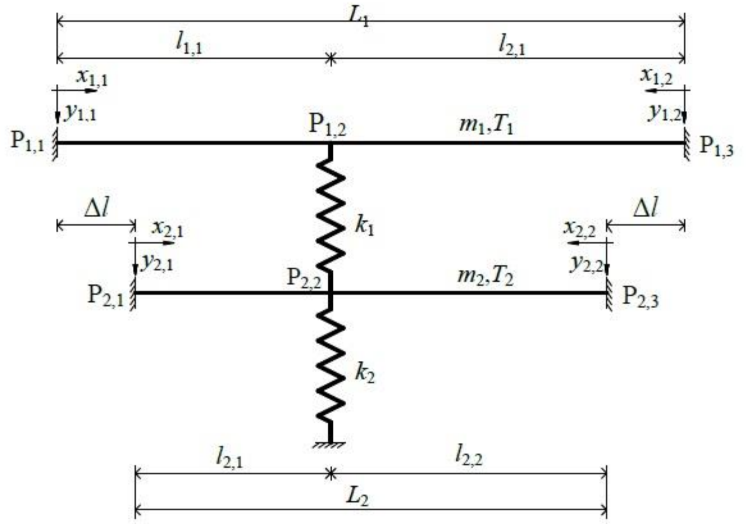

Fig. 1 Two-cable network inter-supported by cross-link fixed to ground

vibration was carried out. Ahmad and Cheng (2016) studied in detail the effects of cross-link stiffness on the dynamics of cable network, considering multiple lines of cross-links with the emphasis on local mode formation of cable networks.

However, most of the above analytical research was based on cable networks without cross-links further extended to ground. In engineering practice, cross-ties are sometimes extended to a deck to further increase system in-plane stiffness (Virlogeux 1998, Kumarasena *et al.* 2007, Bosch and Park 2005). There are only limited studies available discussing the dynamics of cable networks with cross-links extended to ground, most of which correspond to field experiences of cable network design and analysis (Virlogeux 1998, Kumarasena *et al.* 2007, Bosch and Park 2005) or model cable tests (Sun *et al.* 2007, Zhou *et al.* 2017). It is commonly agreed that extending the cross-link to ground would certainly further increase the in-plane stiffness of a cable network. However, the impact on mode behavior was not detailly studied. Caracoglia and Jones (2005a) discussed the dynamics of a two-cable network, and a special case for the cross-link located at the mid-span of the two cables and extended to ground was discussed. An obvious difference of dynamic behaviors was observed between the two-cable network with connection to the ground and that without connection to the ground when the stiffness of the ground connector was high, especially for lower modes of vibration.

Although the extension of cross-ties to ground seems very simple geometrically, it considerably increases the complexity of network behavior and make its analysis very challenging. In this paper, inspired by practical problems and based on previous studies (Caracoglia and Jones 2005a, Ahmad and Cheng 2013), a system of two cables system with cross-link extended to ground is proposed. The proposed system involves connecting two nearby cables by one upper cross-link, and a lower cross-link extended from the upper cross-link to the ground. Although this configuration only adds one cross-link fixed to the ground compared to that of the two-cable system with one inter-connected cross-link, its structural behavior is complex and still not fully understood. An analytical model of this system is developed, and mode evolution with respect to the system configuration and spring stiffness are evaluated to explore the dynamics of the proposed system; which could provide insight and idea of how to implement cross-ties in mitigating the excessive cable vibration.

2. General problem formulation

Fig. 1 shows the proposed system. The two parallel cables are interconnected by an upper transverse spring, where the spring represents the axial stiffness of a cross-link. The second spring under the lower cable is further connected to ground and represents the axial stiffness of a cross-link fixed to the bridge deck/tower. The imperfect orthogonal orientation of the real application of cross-ties can be accounted for by projection of the restoring force and displacement component in the orthogonal direction. The detail steps of the projection were addressed by Caracoglia and Jones (2005b) and not further addressed in this paper.

The length of the j^{th} cable is L_j (j=1,2), with $L_1=L_2+2\Delta l$. T_j is the tension force, m_j is the mass per unit length, the length of the p^{th} segment of the j^{th} cable is denoted as $l_{j,p}$ (p=1,2); its axial coordinate is $x_{j,p}$. The motion equation of each cable segment is (Irvine 1981)

$$m_j \frac{\partial^2 y_{j,p}\left(x_{j,p},t\right)}{\partial t^2} = T_j \frac{\partial^2 y_{j,p}\left(x_{j,p},t\right)}{\partial x_{j,p}^2} \tag{1}$$

where $y_{j,p}(x_{j,p}, t)$ is the transverse displacement and can be expressed as $y_{j,p}(x_{j,p},t)=Y_{j,p}(x_{j,p})e^{i\beta\tau}$, $Y_{j,p}(x_{j,p})$ is the complex mode shape function; $\tau=\omega_1 t$ is the non-dimensional time, where $\omega_1=\pi/L_1\sqrt{T_1/m_1}$ is the fundamental circular frequency of the upper cable, $\beta=\omega/\omega_1$ is the non-dimensional frequency of the system, and ω is the modulus of the non-dimensional eigenvalue.

Considering continuity of displacement, $Y_{j,p}(x_{j,p})$ can be expressed as

$$Y_{j,p}\left(x_{j,p}\right)=A_j\frac{\sin\left(\pi f_j\beta x_{j,p}/L_j\right)}{\sin\left(\pi f_j\beta l_{j,p}/L_j\right)} \tag{2}$$

where $f_j=\omega_1/\omega_j$ is the j^{th} cable frequency ratio (Caracoglia and Jones 2005a, Ahmad and Cheng 2013), $\omega_j=\pi/L_j\sqrt{T_j/m_j}$, and A_j are parameters related to the j^{th} cable vibration amplitude.

Eq. (2) is solved to obtain the unknown amplitudes by means of a set of displacement boundary conditions at the cable ends, displacement continuity equations and force equilibrium equations at the spring locations. Finally, the homogeneous system equations can be re-written in matrix form as $\mathbf{S\Phi=0}$, where $\mathbf{S}$ is a matrix consisting a set of transcendental parameters, and the vector $\mathbf{\Phi}$ includes the unknowns A_j. To get a non-trivial solution ($\mathbf{\Phi}\neq\mathbf{0}$), the determinant of the matrix $\mathbf{S}$ must be zero.

After simplifying the hyperbolic functions, the equation det($\mathbf{S}$)=0 can be re-written as

$$\begin{aligned}&\prod_{j=1}^{2}\left\{\begin{aligned}&\beta\sin\Gamma_j+\gamma_j v_j\sin\left[\Gamma_j\left(\lambda_j\varepsilon_1-\frac{\lambda_j-1}{2}\right)\right]\\&\times\sin\left[\Gamma_j\left(\frac{1+\lambda_j}{2}-\lambda_j\varepsilon_1\right)\right]\end{aligned}\right\}\\&+\gamma_1 v_2\beta\sin\Gamma_1\sin\left[\Gamma_2\left(\lambda_2\varepsilon_1-\frac{\lambda_2-1}{2}\right)\right]\\&\times\sin\left[\Gamma_2\left(\frac{1+\lambda_2}{2}-\lambda_2\varepsilon_1\right)\right]=0\end{aligned} \tag{3}$$

in which $\lambda_j=L_1/L_j$ is the length ratio of the j^{th} cable, $v_j=\sqrt{T_1m_1/T_jm_j}$ is the mass-tension ratio of the j^{th} cable (Caracoglia and Jones 2005a, Ahmad and Cheng 2013), $\gamma_j=k_jL_1/(\pi T_1)$ is the j^{th} non-dimensional cross-link stiffness, $\varepsilon_j=l_{j1}/L_j$ is the position ratio of the cross-link for the j^{th} cable, and $\Gamma_j=\pi f_j\beta$.

For specific values of the system variables, Eq. (3) can be numerically solved for β; then three of the four coefficients in $\mathbf{\Phi}$ can be expressed in terms of the other coefficient, and the mode shape can be obtained from Eq. (2).

3. Limiting solutions

From the above Eq. (3), it can be found that the solutions of the system are dependent on the variables γ_j, v_j, f_j, λ_j and ε_j. Although the total number of variables is actually six considering that $f_1=v_1=\lambda_1=1$, the solutions to Eq. (3) are rather complex, as Eq. (3) is a highly nonlinear transcendental equation. It is impossible to find solutions analytically in closed form for the general case. However, prior to the implementation of the numerical solutions, the special limiting solutions could be categorized with closed form solutions. These special limiting solutions correspond to the boundary of each solution branch for a changing system variable, as discussed in the following.

3.1 Mass-tension ratio v_2 tends to zero

When the mass-tension ratio v_2 tends to zero, Eq. (3) is

$$\begin{aligned}&\left\{\beta\sin\Gamma_1+\gamma_1\sin\left(\Gamma_1\varepsilon_1\right)\sin\left[\Gamma_j\left(1-\varepsilon_1\right)\right]\right\}\\&\times\sin\Gamma_2=0\end{aligned} \tag{4}$$

Eq. (4) includes two sets of roots

$$\beta\sin\Gamma_1+\gamma_1\sin\left(\Gamma_1\varepsilon_1\right)\sin\left[\Gamma_j\left(1-\varepsilon_1\right)\right]=0 \tag{5a}$$

$$\sin\Gamma_2=0 \tag{5b}$$

Eqs. (5(a)) and (5(b)) show that when the mass-tension ratio v_2 tends to zero, the upper cable is inter-supported by a cross-link extended to ground, and the corresponding non-dimensional spring stiffness is γ_1. The lower cable vibrates independently and is not influenced by the cross-link.

3.2 Mass-tension ratio v_2 tends to infinity

When the mass-tension ratio v_2 tends to infinity, Eq. (3) can be re-written as

$$\begin{aligned}&\left\{\beta\sin\Gamma_1+\frac{\gamma_1\gamma_2}{\gamma_1+\gamma_2}\sin\left(\Gamma_1\varepsilon_1\right)\sin\left[\Gamma_1\left(1-\varepsilon_1\right)\right]\right\}\\&\times\sin\left[\Gamma_2\left(\lambda_2\varepsilon_1-\frac{\lambda_2-1}{2}\right)\right]\\&\times\sin\left[\Gamma_2\left(\frac{1+\lambda_2}{2}-\lambda_2\varepsilon_1\right)\right]=0\end{aligned} \tag{6}$$

Eq. (6) includes three sets of roots

$$\beta\sin\Gamma_1+\frac{\gamma_1\gamma_2}{\gamma_1+\gamma_2}\sin\left(\Gamma_1\varepsilon_1\right)\sin\left[\Gamma_1\left(1-\varepsilon_1\right)\right]=0 \tag{7a}$$

$$\sin\left[\Gamma_2\left(\lambda_2\varepsilon_1-\frac{\lambda_2-1}{2}\right)\right]=0 \tag{7b}$$

$$\sin\left[\Gamma_2\left(\frac{1+\lambda_2}{2}-\lambda_2\varepsilon_1\right)\right]=0 \tag{7c}$$

Eqs. (7(a))-(7(c)) show that when v_2 tends to infinity, the upper cable is inter-supported by a cross-link extended to ground, the corresponding non-dimensional spring stiffness equals to that of the two cross-links γ_1 and γ_2 in series. The lower cable is divided into two segments that vibrate independently.

3.3 Non-dimensional spring stiffness tends to zero

It is obvious that γ_2=0 represents the case when there is no cross-link fixed to the ground, and then Eq. (3) can be re-written as

$$\begin{aligned}&\beta\sin(\Gamma_1)\sin(\Gamma_2)\\&+\gamma_1\sin(\Gamma_2)\sin(\Gamma_1\varepsilon_1)\sin[\Gamma_1(1-\varepsilon_1)]\\&+\gamma_1 v_2\beta\sin(\Gamma_1)\sin\left[\Gamma_2\left(\lambda_2\varepsilon_1-\frac{\lambda_2-1}{2}\right)\right]\\&\times\sin\left[\Gamma_2\left(\frac{1+\lambda_2}{2}-\lambda_2\varepsilon_1\right)\right]=0\end{aligned}\tag{8}$$

This case has been studied in detail by Ahmad and Cheng (2013).

When γ_1 equals zero there is no cross-link between the upper and lower cable, and the upper cable is free and the lower cable is inter-supported by a spring, which is a special case discussed by the co-authors when studying a taut cable with a spring and a damper (Zhou *et al*. 2014a).

3.4 Non-dimensional spring stiffness tend to infinity

Three cases should be considered in the following.

3.4.1 Both γ_1 and γ_2 tend to infinity

The first case is that both γ_1 and γ_2 tend to infinity. In this case Eq. (3) can be re-written as

$$\prod_{j=1}^{2}\begin{aligned}&\sin\left[\Gamma_j\left(\lambda_j\varepsilon_1-\frac{\lambda_j-1}{2}\right)\right]\\&\times\sin\left[\Gamma_j\left(\frac{1+\lambda_j}{2}-\lambda_j\varepsilon_1\right)\right]\end{aligned}=0\tag{9}$$

It can be found that the system frequency solutions are composed of 4 sets

$$\sin(\Gamma_1\varepsilon_1)=0\tag{10a}$$

$$\sin[\Gamma_1(1-\varepsilon_1)]=0\tag{10b}$$

$$\sin\left[\Gamma_2\left(\lambda_2\varepsilon_1-\frac{\lambda_2-1}{2}\right)\right]=0\tag{10c}$$

$$\sin\left[\Gamma_2\left(\frac{1+\lambda_2}{2}-\lambda_2\varepsilon_1\right)\right]=0\tag{10d}$$

Eqs. (10(a))-(10(d)) show that when both γ_1 and γ_2 tend to infinity, cross-links act as rigid support; the system was divided into four cable segments that vibrate independently, each set of equations corresponding to the frequency of one of the cables segments.

3.4.2 γ_2 tends to infinity

For the case when γ_2 tends to infinity, Eq. (3) becomes

$$\begin{aligned}&\{\beta\sin\Gamma_1+\gamma_1\sin(\Gamma_1\varepsilon_1)\sin[\Gamma_1(1-\varepsilon_1)]\}\\&\times\sin\left[\Gamma_2\left(\lambda_2\varepsilon_1-\frac{\lambda_2-1}{2}\right)\right]\\&\times\sin\left[\Gamma_2\left(\frac{1+\lambda_2}{2}-\lambda_2\varepsilon_1\right)\right]=0\end{aligned}\tag{11}$$

Eq. (6) is composed of 3 sets of solutions

$$\beta\sin\Gamma_1+\gamma_1\sin(\Gamma_1\varepsilon_1)\sin[\Gamma_1(1-\varepsilon_1)]=0\tag{12a}$$

$$\sin\left[\Gamma_2\left(\lambda_2\varepsilon_1-\frac{\lambda_2-1}{2}\right)\right]=0\tag{12b}$$

$$\sin\left[\Gamma_2\left(\frac{1+\lambda_2}{2}-\lambda_2\varepsilon_1\right)\right]=0\tag{12c}$$

Eqs. (12(a))-(12(c)) show that when γ_2 tends to infinity, the lower cross-link acts as rigid support, the upper cable is inter-supported by the upper cross-link extended to ground, and the lower cable is divided into two segments.

3.4.3 γ_1 tends to infinity

For the case when γ_1 tend to infinity and γ_2 is finite, Eq. (3) can be simplified as

$$\begin{aligned}&\gamma_2 v_2\sin(\Gamma_1\varepsilon_1)\sin[\Gamma_1(1-\varepsilon_1)]\\&\times\sin\left[\Gamma_2\left(\lambda_2\varepsilon_1-\frac{\lambda_2-1}{2}\right)\right]\sin\left[\Gamma_2\left(\frac{1+\lambda_2}{2}-\lambda_2\varepsilon_1\right)\right]\\&+\beta\sin\Gamma_2\sin(\Gamma_1\varepsilon_1)\sin[\Gamma_1(1-\varepsilon_1)]\\&+v_2\beta\sin\Gamma_1\sin\left[\Gamma_2\left(\lambda_2\varepsilon_1-\frac{\lambda_2-1}{2}\right)\right]\\&\times\sin\left[\Gamma_2\left(\frac{1+\lambda_2}{2}-\lambda_2\varepsilon_1\right)\right]=0\end{aligned}\tag{13}$$

Eq. (13) is still complex and cannot be further simplified. However, study shows that for a special case of a twin cable system, which refers to the two identical cables, Eq. (13) can be re-written as

$$\begin{aligned}&\sin(\Gamma_1\varepsilon_1)\sin[\Gamma_1(1-\varepsilon_1)]\\&\times\{\beta\sin\Gamma_1+\gamma_2/2\sin(\Gamma_1\varepsilon_1)\sin[\Gamma_1(1-\varepsilon_1)]\}=0\end{aligned}\tag{14}$$

Eq. (14) could be further re-written as

$$\sin(\Gamma_1\varepsilon_1)=0\tag{15a}$$

$$\sin[\Gamma_1(1-\varepsilon_1)]=0\tag{15b}$$

$$\beta\sin\Gamma_1+\gamma_2/2\sin(\Gamma_1\varepsilon_1)\sin[\Gamma_1(1-\varepsilon_1)]=0\tag{15c}$$

Eqs. (15(a))-(15(c)) show that when γ_1 tends to infinity, the characteristic equation of a twin-cable system contains three sub-equations, the first two sub-equations correspond to

Table 1 Properties of the limiting solutions

Limiting cases	Eqns. No.	Solution properties
$v_2\to 0$	(5a) (5b)	1. The upper cable is inter-supported by a cross-link extended to ground; 2. The lower cable vibrates independently.
$v_2\to\infty$	(7a) (7b) (7c)	1. The upper cable is inter-supported by a cross-link extended to ground; 2. The lower cable is divided into two segments that vibrate independently.
$\gamma_2\to 0$	(8)	This case has been studied in detail by Ahmad and Cheng (2013).
$\gamma_1\to\infty$, $\gamma_2\to\infty$	(10a) (10b) (10c) (10d)	1. The cross-links acts as rigid support; 2. The system is divided into four cable segments.
$\gamma_2\to\infty$	(12a) (12b) (12c)	1. The lower cross-link acts as rigid support; 2. The upper cable was inter-supported by a cross-link extended to ground; 3. The lower cable is divided into two segments.
$\gamma_1\to\infty$ for twin cable system	(15a) (15b) (15c)	1. The first two equations corresponds to vibration of the two cable segments; 2. The other corresponds to a cable supported by a spring.

vibration of the two cable segments, the other corresponds to the cable supported by a spring, so that the stiffness was actually only half of the lower spring's, as the lower spring now actually connects two cables in the system.

The above studies show that, taking into the simplification of cable parameters, the solutions of the system characteristic equation still can be further simplified. In the following, a collection of some relevant examples is constructed, for the purpose of better identifying the system's physical behaviours and revealing its intrinsic characteristics. According to the above discussion, the properties of limiting solutions are summarized in Table 1.

4. Applications to cable systems with special configurations

4.1 Two identical cables

For the twin cable system, Eq. (3) could be re-written as

$$\prod_{j=1}^{2}\left\{\beta\sin\Gamma_1+\gamma_j\sin\left(\Gamma_1\varepsilon_1\right)\sin\left[\Gamma_1\left(1-\varepsilon_1\right)\right]\right\}$$
$$+\gamma_2\beta\sin\Gamma_1\sin\left(\Gamma_1\varepsilon_1\right)\sin\left[\Gamma_1\left(1-\varepsilon_1\right)\right]=0 \quad (16)$$

It can be found that Eq. (16) is much more complex than that for an interconnected twin cable system without cross-link to ground (Ahmad and Cheng 2013); the added term with γ_2 shows the effects of the cross-link extended to the ground. The following discusses the special case of a cross-link located at the quarter span, for comparison with the results of Ahmad and Cheng (2013).

Fig. 2 shows the first 4 mode shapes and frequencies of system with 4 different sets of non-dimensional stiffness of the cross-link: $\gamma_1=\gamma_2=0.1$, $\gamma_1\to\infty$ and $\gamma_2=0.1$, $\gamma_1=0.1$ and $\gamma_2\to\infty$, $\gamma_1=\gamma_2=10$. The set of cross-link stiffness was selected to show the effects of the cross-link and to compare with the analytical results, as Eqs. (12) and (15) shows the analytical closed form solutions.

Comparing the frequencies in Fig. 2(a)-2(c) showed that it was effective to increase the even mode of vibration frequency by increasing γ_1 or γ_2 individually; however, it also showed that it was inefficient to increase the odd mode of vibration frequency by increasing γ_1 or γ_2 separately for the twin cable system. The corresponding mode shape in Fig. 2 shows that the even and odd modes of vibration corresponds to the in-phase and out-of-phase modes of vibration for a finite γ_2.

Comparison of the roots of $\gamma_1=\gamma_2=0.1$ to that of $\gamma_1=\gamma_2=10$ showed that it was efficient to increase both the even and odd modes of vibration frequencies by increasing the non-dimension stiffness of the upper and lower cross-link together.

For finite cross-link stiffness, Fig. 2 shows that increasing cross-link stiffness would enhance the constraint between the two end points of the cross-link. Comparison of Fig. 2(b) to Fig. 2(c) clearly shows the different effects of the two cross-links, as the upper cross-link restrains the two points $P_{1,2}$ of the upper cable and $P_{2,2}$ of the lower cable, however, the lower cross-link only restrains the point $P_{2,2}$ of the lower cable.

Fig. 2 also clearly shows the emergence of the local mode of vibration for the infinite cross-link stiffness cases. The difference was attributed to the above: the local modes corresponding to $\gamma_1\to\infty$ are the out-of-phase modes of vibration, and $P_{1,2}$ and $P_{2,2}$ acted as the immobile points of cable segment; however, the local modes corresponding to $\gamma_2\to\infty$ are the single mode of vibration of the upper cable or segment of the lower cable, as $P_{2,2}$ were acting as the immobile points.

To assess the distinction between the global and local modes, Ahmad and Cheng (2016) give a definition for the degree of mode localization by vibration amplitude of cable segments; however, the potential energy of each cable segment gives a more reasonable way of distinguishing between the global mode and local mode. The following gives the variables used to assess the degree of mode localization by energy distribution of each cable segment.

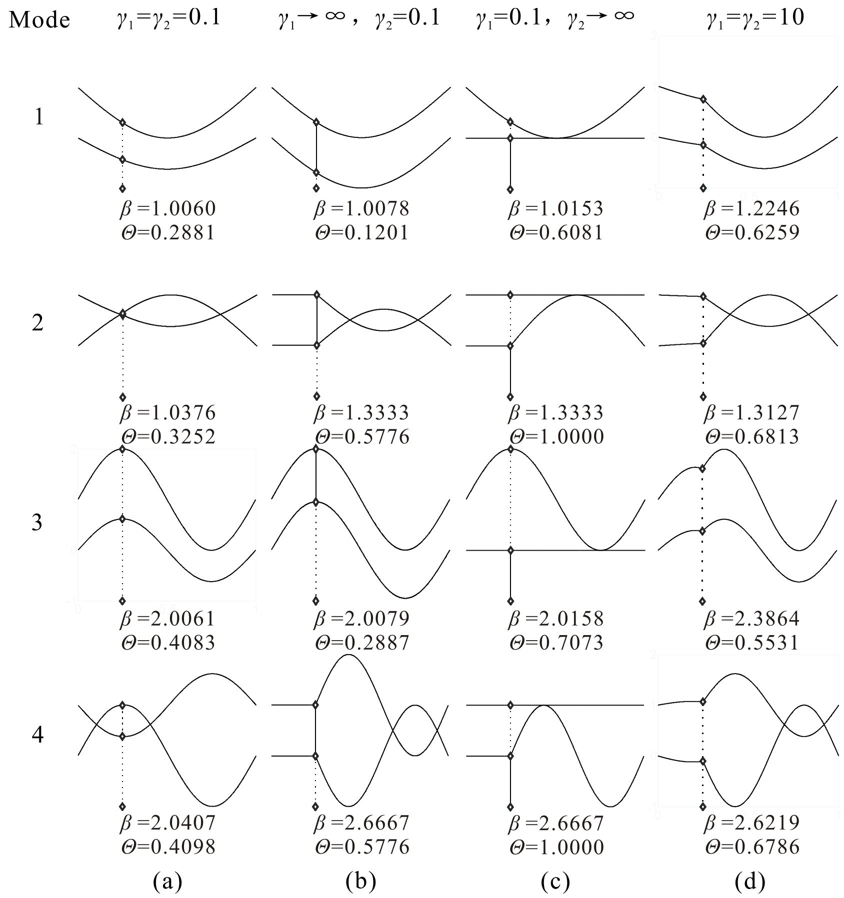

Fig. 2 Mode shapes of the first four mode of twin cable system

The mode energy distribution vector was firstly defined as

$$\mathbf{E} = \left[E_{11}\ E_{12}\ E_{21}\ E_{22}\right] \tag{17}$$

where E_{j1} and E_{j2} are the non-dimensional potential vibration mode energies of the cable segments $P_{j,1}$ to $P_{j,2}$ and $P_{j,2}$ to $P_{j,3}$. These can be derived by calculating the potential vibration mode energy from the known mode shape (Eq. (2)), as shown in the Appendix.

The mode energy distribution vector could clearly show the vibration mode energy distribution of each segment; however, it cannot give a simple and direct way to identify the "global" and "local" mode. It is certain that if the energy is well-distributed in the four cable segments, the vibration mode is "global", however, when the energy is concentrated on only one cable segment, the vibration mode is extremely "local". Recognizing the above phenomenon, it is natural to adopt the non-dimensional coefficient of variation of the four non-dimensional potential vibration mode energies of the cable segments as the index by which to measure the degree of mode localization

$$\Theta = \sqrt{\frac{N}{N-1}}\sqrt{\sum_{j=1}^{2}\sum_{p=1}^{2}\left(E_{jp}-\frac{1}{N}\right)^2} = \sqrt{\frac{4}{3}}\sqrt{\sum_{j=1}^{2}\sum_{p=1}^{2}\left(E_{jp}-\frac{1}{4}\right)^2} \tag{18}$$

where N is the total number of cable segments, N=4 in this paper. It should be noted that for single cable segment vibration, only one element of the vector E equal to one and the other element is zero, and this happens for Θ=1.0; when each cable segment has the same vibration energy, then E_{jp}=1/4 and Θ=0. There is also a special case for two cable segments vibration with the same energy with other cable elements do not vibrate, and then $\Theta=1/\sqrt{3}\approx 0.577$.

It could be concluded that the vibration mode would be more "local" as Θ increases. The value of Θ are also listed in Fig. 2, a clear identification of local mode when Θ is greater than 0.5 for the listed mode shapes.

Fig. 3 further shows the non-dimensional frequency of the first 4 modes as the cross-link moves from the left anchorage to the middle, only half of cable system is shown due to the fact of symmetry. The non-dimensional cross-link stiffness was selected as $\gamma_1=\gamma_2$, and four different levels: 0.1, 1, 10 and 100 were selected for analysis. Figs. 3(a) and 3(b) shows the increment of non-dimensional frequency as the cross-link moves from the left end to the middle of the cable, a larger stiffness of the cross-link leads to a larger increment of frequency. Figs. 3(c) and 3(d) show the same tendency as the cross-link stiffness increases, but there is a kink. The location of this kink is skewed to the right as the non-dimensional cross-link stiffness increases, and reaches about $\varepsilon_1=\varepsilon_2$=1/3 when γ=100, which corresponds to the emergence of a local mode.

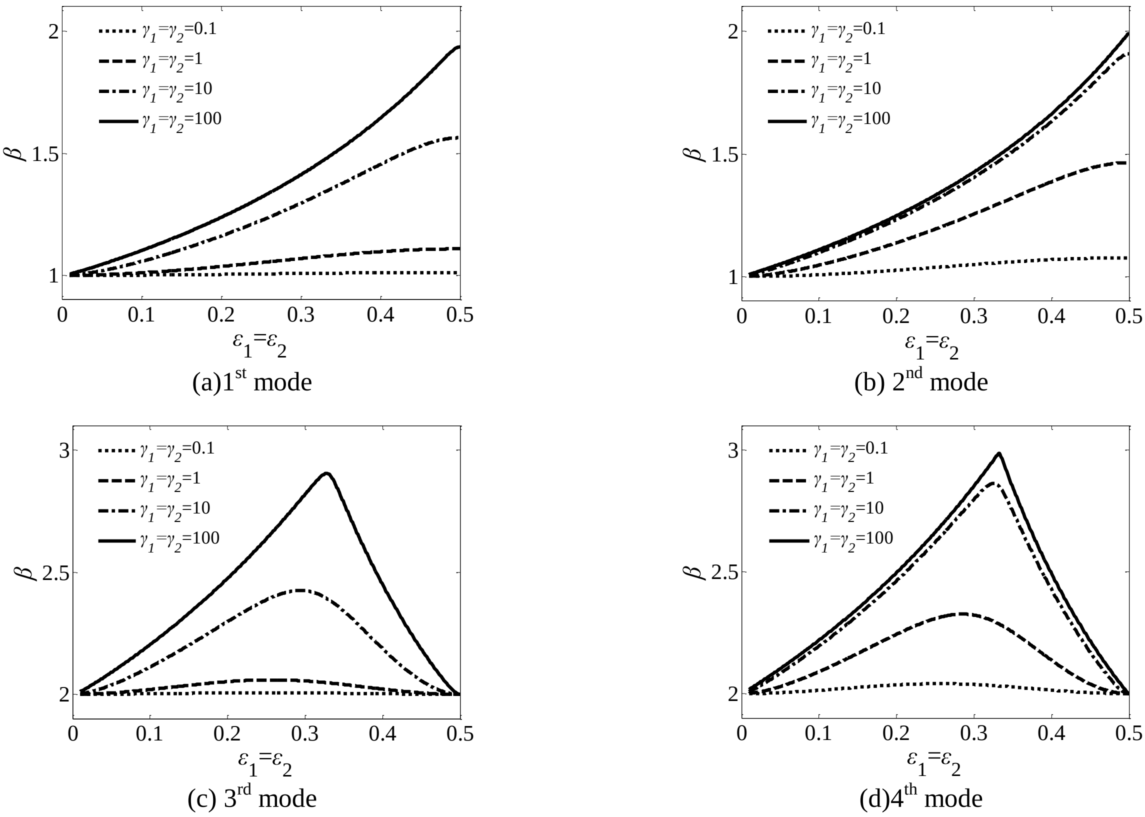

Fig. 3 Non-dimensional frequency vs. position ratio (ε_1,ε_2) (γ_1=γ_2, twin cables)

Fig. 4 shows the evolution of the 3rd mode shape for the non-dimensional cross-link stiffness equal to 0.1, 1, 10 and 100; the cross-link location was selected as ε_1=ε_2=0.25 and ε_1=ε_2=0.35 to illustrate the difference in frequency shown above. The emergence of a local mode of cable vibration could be obviously observed as γ increases for the two cross-link locations. However, there was also an obvious difference between the two different local modes: the right segment of cable vibration arises for ε_1=ε_2=0.25 while the left segment arises for ε_1=ε_2=0.35. The observations could well explain the kink as stated above; the frequency was determined by Eq. (10(a)) for the left cable segment vibration, while Eq. (10(b)) for the right cable segment. Fig. 4 also shows that Θ also changes differently for these two cross-link locations, it increases monotonically as the cross-link stiffness increases when ε_1=ε_2=0.25; however, it further decreases and then increases again when ε_1=ε_2=0.35. The mode shape in Fig. 4 also clearly shows the vibration energy flow from the right segment to the left segment of the two cables as the cross-link stiffness increases. An interesting point is that the above observation showed that the system vibration would not be certainly more "local" as the cross-link stiffness increases. On the contrary, there is a limit cross-link stiffness such that the system vibration mode is mostly "global" when ε_1=ε_2=0.35.

Further investigation shows that the above phenomenon was determined by cross-link locations and cable vibration mode number. When $\varepsilon \in \left(\frac{i}{n}, \frac{2i+1}{2n}\right]$, Θ will increases monotonically as the cross-link stiffness increases and approaches a certain value, where n is the single cable vibration mode number and n=1,2,3,...; i=0,1,2,... and $i \le n/2$. The vibration mode changes gradually from "global" to "local" as the non-dimensional cross-link stiffness increases. Fig. 5 shows the increase of Θ as the non-dimensional cross-link stiffness increases for the third mode (2nd mode for a single cable) vibration when ε_1=ε_2=0.15 and ε_1=ε_2=0.25. When $\varepsilon \in \left(\frac{2i+1}{2n}, \frac{i+1}{n}\right)$, Θ decreases at first and then increases as the cross-link stiffness increases. Fig. 5 also shows the case for the third mode (2nd mode for a single cable) vibration when ε_1=ε_2=0.35 and ε_1=ε_2=0.45. There was a limit to the non-dimensional cross-link stiffness corresponding to the smallest Θ.

Further study shows that the above phenomena are related to opposite vibration energy flow as the non-dimensional cross-link stiffness increases: when $\varepsilon \in \left(\frac{i}{n}, \frac{2i+1}{2n}\right]$, vibration energy flows from the left segments to the right segments; however, when $\varepsilon \in \left(\frac{2i+1}{2n}, \frac{i+1}{n}\right)$, vibration energy flows from the right segments to the left segments.

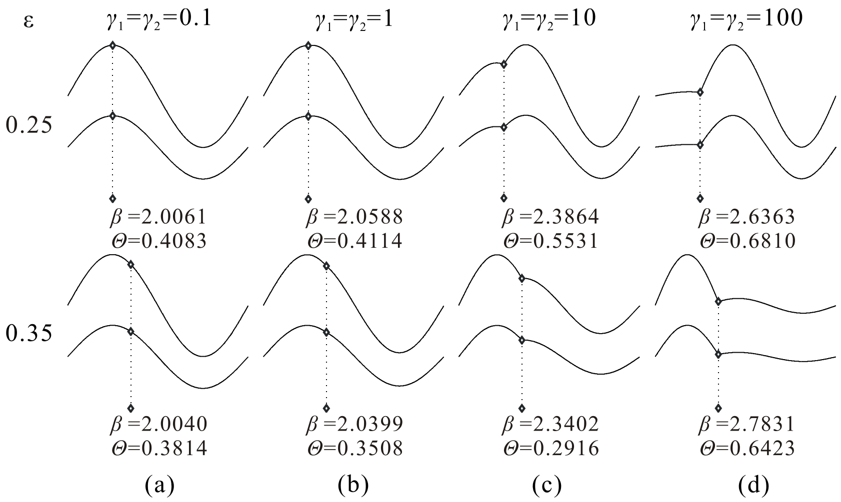

Fig. 4 Evolution of the 3rd mode shape (twin cables, $\varepsilon_1=\varepsilon_2=0.25$ and $\varepsilon_1=\varepsilon_2=0.35$)

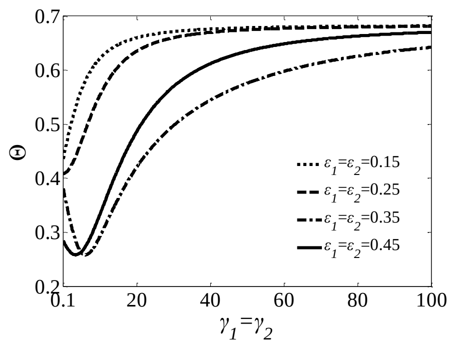

Fig. 5 Evolution of Θ as cross-link stiffness increases for 3rd (2nd in-phase) mode vibration of twin cable system

As the left segments are shorter than right segments, the vibration energy of the left segments is smaller than that of the right segments when the non-dimensional cross-link stiffness is small. Vibration would be more "local" when energy flows from left to right; however, the vibration would become more "global" when energy flows from right to left, and there is the limit to the non-dimensional cross-link stiffness corresponding to the most well-distributed vibration energy. Further studies show this limit cross-link stiffness value depends on the location and mode number and can only be calculated by numerical iteration. When $\varepsilon_1=\varepsilon_2=(i+1)/n$, the cross-link has no effects on the system, since it lies on the node of the vibration mode shape.

The above studies clearly show that the twin cable system frequency would increase as the two cross-link stiffness increase. When the upper and lower cross-link stiffness were the same, there is a kink for non-dimensional frequency curves as the cross-link moves from the left end of the cable to the middle. The location of this kink is approaching $i/(n+1)$ as the non-dimensional cross-link stiffness increases for the n^{th} mode of cable vibration ($(2n)^{th}$ or $(2n+1)^{th}$ mode of a twin cable system vibration), and the upper limit of the non-dimensional frequency is $n+1$; these limits are determined by the limiting solution of Eq. (10).

When two cross-link stiffness were both small, the mode behaviour was "global" as four segments and cable all vibrated obviously, and a distinction between the in-phase and the following out-of-phase mode of vibration could be found for each of the two sets of twin cable vibrations. When the upper cross-link stiffness was large and tend to infinity while the lower cross-link stiffness was finite, the local mode of vibration arose for the out-of-phase mode of vibration. When the lower cross-link stiffness was large and tended to infinity with the upper cross-link stiffness being finite, the individual vibrations of the upper cable or the two segments of lower cable arose.

4.2 Two unequal length cables

The above text gives the mode behaviours of a twin cable network, but the cable parameters might be different in engineering practice. In what follows, further investigation on two unequal length cables was made. The length ratio λ_2=1.25, frequency ratio f_2=0.8 and the mass-tension ratio was unitary according to reference (Ahmad and Cheng 2013). Figs. 6 and 7 show the first 4 mode shapes and the corresponding β and Θ when the non-dimensional cross-link stiffness was selected as $\gamma_1=\gamma_2$ for four different levels: 0.1, 1, 10 and 100, and the cross-link

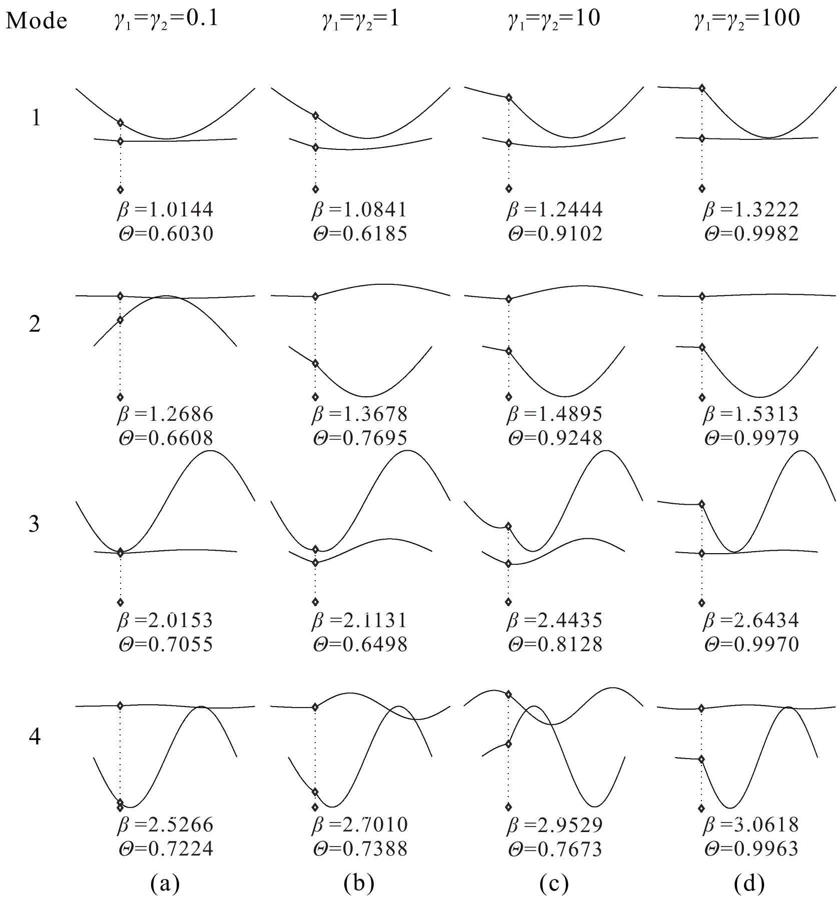

Fig. 6 Mode shapes of the first four mode of two unequal cables (λ_2=1.25, f_2=0.8, v_2=1, ε_1=0.25, ε_2=0.1875)

location was selected as ε_1=0.25 (ε_2=0.1875) and 0.35 (ε_2=0.3125), respectively.

Fig. 6(a) shows that for the cross-link stiffness $\gamma_1=\gamma_2$=0.1, the connection between the two different cables was weak, the two unequal cables vibrated almost independently, and the index of mode localization was greater than $1/\sqrt{3} \approx 0.577$ when the two segments of one cable were about 1:3 in length. Also, the vibration frequency appeared to be well-sequenced and slightly greater than that of a free cable. In Fig. 6(b) there appears a coupling of the two unequal cable vibrations at $\gamma_1=\gamma_2$=1; the mode shape and the corresponding frequency were still well-sequenced and moderately larger than that of a free cable. Different from twin cable system, the value of Θ decreases significantly for the 3rd mode, which shows more “global” mode behaviour. Actually, Θ increases for the 1st, 2nd and 4th modes as the non-dimensional cross-link stiffness increases. Fig. 6(c) corresponds to two unequal cable vibration when $\gamma_1=\gamma_2$=10. It shows the 1st to 4th modes of vibration become dominated by the right segment of the upper and lower cable segments vibration. The value of Θ is increased significantly compared to that when $\gamma_1=\gamma_2$=1. Fig. 6(d) shows full emergence of localized cable segment vibration as $\gamma_1=\gamma_2$=100, all mode shapes show only one segment cable vibration.

Fig. 7(a) shows that for the cross-link stiffness $\gamma_1=\gamma_2$=0.1, the two unequal cables still vibrated almost independently, but Θ was near to 0.577 as the length ratio of the two cable segments were close to 1 as compared to that seen in Fig. 6(a). Fig. 7(b) shows the coupling of two unequal cable vibrations when $\gamma_1=\gamma_2$=1; the mode shape and the corresponding frequency were still well-sequenced and moderately larger than that of a free cable. Different from that of twin cable systems, the value of Θ decreases significantly for the 1st mode, which shows a more “global” mode behaviour as the non-dimensional cross-link stiffness increases. The 2nd, 3rd and 4th modes showed the same changing pattern for Θ as the non-dimensional cross-link stiffness increases. Fig. 7(c) corresponds to two unequal cable vibrations at $\gamma_1=\gamma_2$=10. The value of Θ is increased comparing to that of $\gamma_1=\gamma_2$=1 except for the 3rd mode, where it slightly decreases from 0.5520 to 0.5212. Fig. 7(d) shows the full emergence of localized cable segment vibration as $\gamma_1=\gamma_2$=100.

Figs. 6 and 7 show that the vibration of two unequal cables would be more “local” than that of a twin cable system, because Θ of the system of two different cables is significantly larger than that for a twin cable system. It could also be confirmed that a larger cross-link stiffness is required to connect two different cables and vibrate together, as Figs. 6(a) and 7(a) show nearly a single cable vibration for the case of $\gamma_1=\gamma_2$=0.1, as compared to global mode vibration of the twin cable system (Fig. 2(a)). It can be concluded that the vibration would not be certainly more “local” as cross-link stiffness increases; on the contrary, it

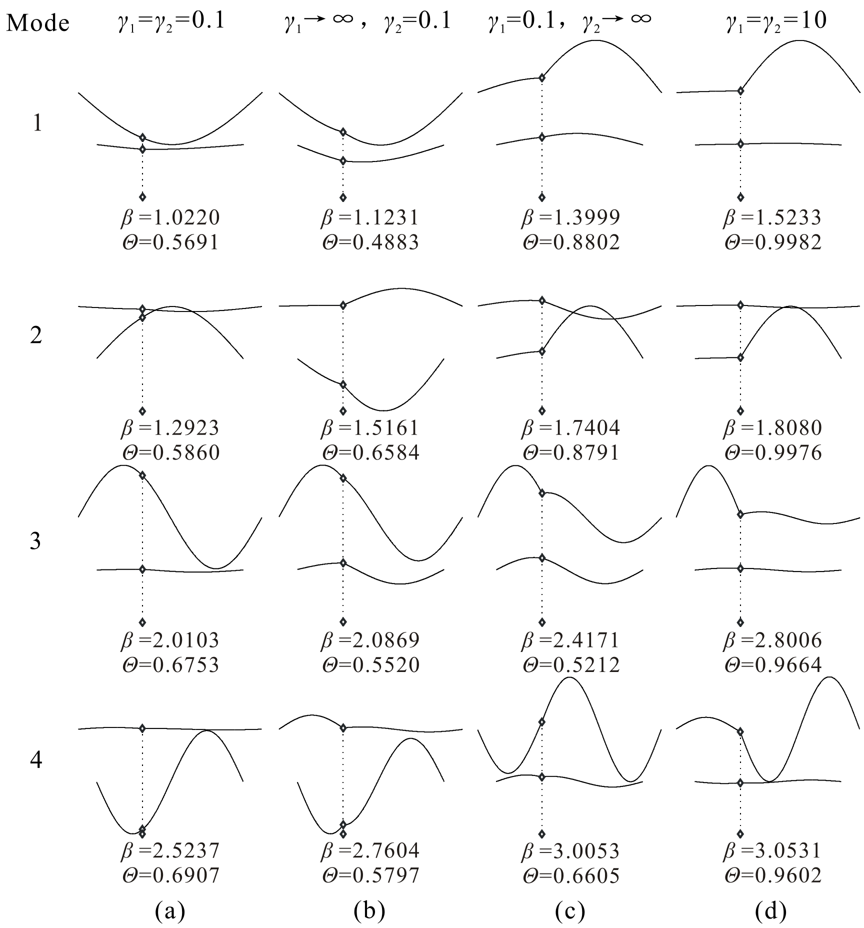

Fig. 7 Mode shapes of the first four mode of two unequal cables (λ_2=1.25, f_2=0.8, v_2=1, ε_1=0.35, ε_2=0.3125)

could be more "global" for some specific cross-linklocations, mode numbers and cross-link stiffness values. It could also be concluded that there is a significant difference of vibration mode as the parameters of the system change. Comparing Fig. 2(a) to Fig. 6(a) also shows an increment of frequency for two unequal cables as compared to twin cables. Parametric studies were carried out to address this point in the following.

5. Parametric studies

In this section, the parameters affecting the 1st mode in-plane non-dimensional frequency of a cable network with flexible cross-links will be discussed. These system parameters are the length ratio λ_2, the position ratio ε_1, the frequency ratio f_2, the mass-tension ratio v_2, and the cross-link stiffness ratio γ_2/γ_1. When length ratio, position ratio, frequency ratio and mass-tension ratio were studied, four different cross-link stiffness were selected, γ_1=γ_2=0.1, 1.0, 10 and 100, representing four different types of cross-links, as stated above. While the cross-link stiffness ratio was studied, the upper cross-link stiffness was γ_1=0.1, 1.0, 10 and 100. The other parameters were taken to be the same as those from Cheng and Ahmad (2013) so as to make the appropriate comparisons and study the effects of the lower cross-link fixed to ground.

5.1 Length ratio

Fig. 8 shows the change of the 1st mode non-dimensional frequency as the length ratio λ_2 varies from 1 to 2, when the upper cross-link is located at the quarter span of the upper cable, the frequency ratio f_2=0.667 and the mass-tension ratio v_2=1. Non-dimensional frequency increases as length ratio increases, this trend being the same as the system of two cables with one cross-tie studied by Cheng and Ahmad (2013). However, there is one very small difference. Fig. 8 shows that the increments of non-dimensional frequency are 0.1%, 2.2%, 2.8% and 0.5% when the non-dimensional cross-link stiffness are 0.1, 1.0, 10 and 100, respectively, this as the length ratio increases from 1 to 2. However, the increment increases monotonically as reported in (Ahmad and Cheng 2013). It could also concluded that the length ratio only had a tiny effect on the 1st mode non-dimensional frequency. Further study shows that the effects of length ratio decrease as the cross-link position moves from 1/4 span to 1/2 span, and when a cross-link was installed at 1/2 span, the 1st mode non-dimensional frequency was independent of the length ratio. This phenomenon was the same as that observed in Cheng and Ahmad's (2013) studies.

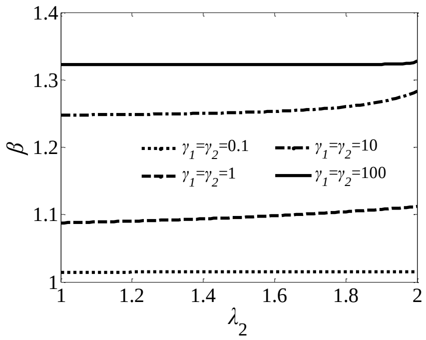

Fig. 8 Non-dimensional frequency vs. length ratio (λ_2)(ε_1=0.25, f_2=0.667, v_2=1, λ_2=1~2)

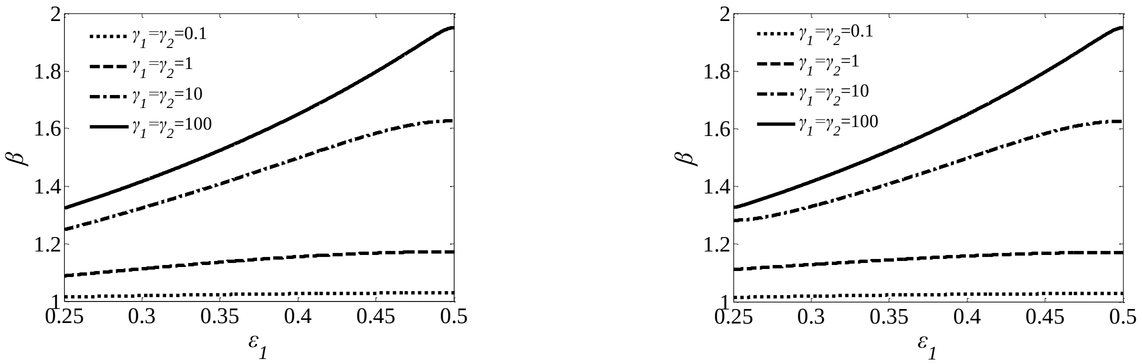

(a) λ_2=1

(b) λ_2=1.8

Fig. 9 Non-dimensional frequency vs. position ratio (ε_1) (f_2=0.667,v_2=1,ε_1=0.25~0.5)

5.2 Position ratio

Fig. 9(a) shows the change of the 1st mode non-dimensional frequency as the position ratio varies from 0.25 to 0.5, when frequency ratio f_2=0.667, mass-tension ratio v_2=1 and length ratio λ_2=1. It clearly shows an increasing trend for non-dimensional frequency as the position ratio increases. The increment of non-dimensional frequency increases monotonically as the cross-link stiffness increases. Fig. 9 shows that the increment of non-dimensional frequency is 1.4%, 7.7%, 30.3% and 47.4% when the non-dimensional cross-link stiffness is 0.1, 1.0, 10 and 100, respectively, as the position ratio increases from 0.25 to 0.5. It could also be concluded that when the cross-link stiffness is large, the position ratio had substantial effects on the non-dimensional frequency. There is some difference as compared to Cheng and Ahmad's (2013) studies, as can be seen in Fig. 9(b); the effect on the position ratio changes is negligible as the length ratio increases from 1 to 1.8; but in Cheng and Ahmad's (2013) studies, it changes significantly when the cross-link stiffness is large.

5.3 Frequency ratio

Fig. 10 shows the change of the 1st mode non-dimensional frequency as the frequency ratio varies from 0 to 1, when cross-links are located at 1/3 span, the mass-tension ratio v_2=1 and length ratio λ_2=1.2. It clearly shows a decreasing trend for the non-dimensional frequency as the frequency ratio increases; this trend was the same as observed by Cheng and Ahmad (2013). However, Fig. 10 shows the decrement does not increase monotonically when the cross-link stiffness increases; while Cheng and Ahmad (2013) reported that non-dimensional frequency decreased gradually and the decrement of non-dimensional frequency increases monotonically as the cross-link stiffness increases. The non-dimensional frequency decrease 0.014, 0.094, 0.104 and 0.072 when the non-dimensional cross-link stiffness are 0.1, 1.0, 10 and 100 as frequency ratio increases from 0 to 1. When cross-link stiffness is large (γ_1=γ_2=10, 100), the curves could be divided into two stages, the first stage is relative flat when the frequency ratio increase from 0 to 0.9, while the second stage is a rapid descending branch when the frequency ratio increase from 0.9 to 1. Further study shows the effects of frequency ratio decreases as cross-link position moves from 1/3 span to 1/2 span, and when cross-link was installed at 1/2 span, the effects of frequency ratio was insignificant.

5.4 Mass-tension ratio

Fig. 11 shows the change of 1st mode non-dimensional frequency as mass-tension ratio varies from 0 to 2 when cross-links are located at 1/4 span, length ratio λ_2=1.2 and frequency ratio f_2=0.833.

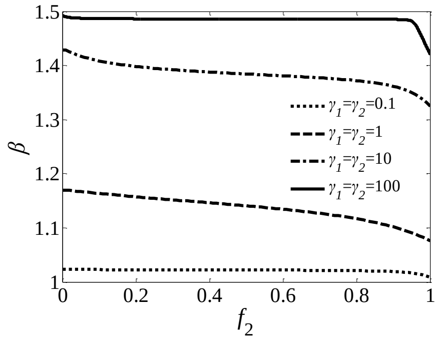

Fig. 10 Non-dimensional frequency vs. frequency ratio (f_2)(ε_1=1/3, v_2=1, λ_2=1.2, f_2=0~1)

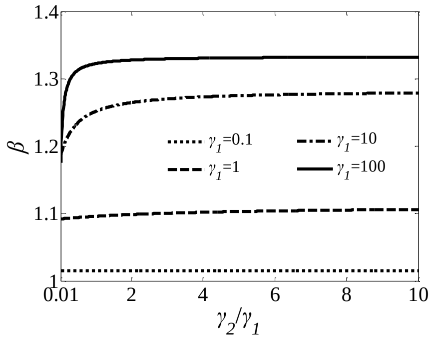

Fig. 12 Non-dimensional frequency vs. cross-link stiffness ratio (γ_2/γ_1)(ε_1=0.25, λ_2=1.5, f_2=0.667, v_2=1, γ_2/γ_1=0.01~10)

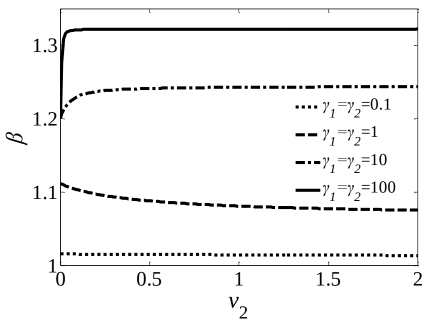

Fig. 11 Non-dimensional frequency vs. mass-tension ratio (v_2)(ε_1=0.25, λ_2=1.2, f_2=0.833, v_2=0~2)

The variation of non-dimensional frequency as mass-tension ratio increases was quite different from the system of two cables with one inter-link (Ahmad and Cheng 2013) in which the decrement of non-dimensional frequency increases monotonously as cross-link stiffness increases. The four curves are divided into two groups, with these corresponding to cross-link stiffness $\gamma_1=\gamma_2$ =0.1 and 1 show the decreasing trend, while the $\gamma_1=\gamma_2$ =10 and 100 show the increasing trend. Studies reveals the non-dimensional frequency and mode shape of the system are nearly independent from the mass-tension ratio when cross-link stiffness $\gamma_1=\gamma_2$ are around 5.7. The decreasing trend or increasing trend is obvious as mass-tension ratio increases from 0 to 0.5 and there is a relative flat as mass-tension ratio increases from 0.5 to 2. Further study shows the effects of mass-tension ratio change little as cross-link position moves from 1/4 span to 1/2 span of the upper cable.

5.5 Cross-link stiffness ratio

Fig. 12 shows the change of 1st mode non-dimensional frequency as cross-link stiffness ratio varies from 0.01 to 100 when cross-links are located at 1/4 span, length ratio λ_2=1.5, frequency ratio f_2=0.667 and mass-tension ratio v_2=1. It clearly shows an increasing trend for non-dimensional frequency as cross-link stiffness ratio increases. As the non-dimensional upper cross-link stiffness increases, the increment of the non-dimensional frequency increases monotonically.

Fig. 12 shows that when the upper cross-link stiffness is small (γ_1= 0.1, 1), the effect of the cross-link stiffness ratio on non-dimensional frequency is not obvious. For an increased upper cross-link stiffness (γ_1= 10, 100), the effect of the cross-link stiffness ratio on the non-dimensional frequency is more obvious, especially when the cross-link stiffness ratio increases from 0.01 to 3. Fig. 12 shows that the increment of the non-dimensional frequency is 6.7% and 10.3% when the non-dimensional upper cross-link stiffness are 10 and 100 and the cross-link stiffness ratio increases from 0.01 to 3. Further, the effects of cross-link stiffness ratio change little as the cross-link's position moves from 1/4 span to 1/2 span.

Comparing with the system of two cables with one inter-link (Ahmad and Cheng 2013), it could be concluded that the effects of system parameters on the 1st mode in-plane non-dimensional frequency are different, especially for the position ratio and mass-tension ratio. Increasing length ratio, position ratio and cross-link stiffness ratio, or decreasing frequency ratio, could improve the 1st mode in-plane non-dimensional frequency. The frequency and mode shape was nearly independent from the mass-tension ratio for a typical cross-link stiffness value; this phenomenon was also not observed for a two cables system with one cross-link (Ahmad and Cheng 2013).

6. Conclusions

This paper investigated vibration characteristics of a system of two-cables connected by an inter-supported cross-link with a lower cross-link extended to ground. The following conclusions could be drawn based on the above work:

(1) For the system of two identical cables, it was effective to increase the even mode of the vibration frequency by increasing γ_1 or γ_2 individually. However, it was inefficient to increase the odd mode of vibration frequency by increasing γ_1 or γ_2 separately.

(2) The vibration mode becomes local when the non-dimensional spring stiffness increases and approaches

infinity; however, mode does not always change from "global" to "local" monotonically as cross-link stiffness increases. For a system of two identical cables, Θ may increase monotonically or Θ may decrease at first and then increase as the cross-link stiffness increases in certain locations.
(3) The frequency increases monotonically when the two equal cross-links stiffness increases for twin cable system. It also varies in a predictable manner when the position ratio changes.
(4) The vibration of two unequal cables system is more "local" than the vibration of a system of two identical cables, and it needs a larger cross-link stiffness to connect two different cables and vibrate together. The mode evolution becomes much more complex than that of the twin cables system for a system of two unequal cables.
(5) The length ratio only had a tiny effect on the 1st mode non-dimensional frequency. For other system parameters: position ratio, frequency ratio, mass-tension ratio and cross-link stiffness ratio, when the cross-link stiffness was small, their effects were small. While using the more rigid cross-link, they played more important roles in affecting the 1st mode in-plane non-dimensional frequency. It was also found that the effects of system parameters on the 1st mode in-plane non-dimensional frequency is a bit different from the system without a lower cross-link.

Acknowledgments

The work described in this paper was financially supported by the National Natural Science Foundation of China (Grant Nos. 51578336 & 51108269), Shenzhen Knowledge Innovation Plan Project (Grant No. JCYJ20170818102511790) and the Ministry of Science and Technology for the 973-project (No. 2011CB013604).

References

Ahmad, J. and Cheng, S.H. (2013), "Effect of cross-link stiffness on the in-plane free vibration behaviour of a two-cable network", *Eng. Struct.*, **52**, 570-580. https://doi.org/10.1016/j.engstruct.2013.03.018.
Ahmad, J., Cheng, S.H. and Ghrib, F. (2016), "Impact of cross-tie design on the in-plane stiffness and local mode formation of cable networks on cable-stayed bridges", *J. Sound Vib.*, **363**, 141-155. https://doi.org/10.1016/j.jsv.2015.09.052.
Bosch, H.R. and Park, S.W. (2005), "Effectiveness of external dampers and cross-ties in mitigation of stay cable vibrations", *Proceedings of the 6th International Symposium on Cable Dynamics*, 2005, Charleston, South Carolina, US.
Caracoglia, L. and Jones, N.P. (2005a), "In-plane dynamic behavior of cable networks. Part 1: formulation and basic solutions", *J. Sound Vib.*, **279**(3-5), 969-991. https://doi.org/10.1016/j.jsv.2003.11.058.
Caracoglia, L. and Jones, N.P. (2005b), "In-plane dynamic behavior of cable networks. Part 2: prototype prediction and validation", *J. Sound Vib.*, **279**(3-5), 993-1014. https://doi.org/10.1016/j.jsv.2003.11.059.
Chen, Z.Q., Wang, X.Y., Ko, J.M., Ni, Y.Q., Spencer, B.F., Jr., Yang, G. and Hu, J.H. (2004), "MR damping system for mitigating wind-rain induced vibration on Dongting Lake Cable-Stayed Bridge", *Wind Struct.*, **7**(4), 293-304. http://dx.doi.org/10.12989/was.2004.7.5.293.
Christenson, R.E., Spencer, B.F. and Johnson, E.A. (2006). "Experimental verification of smart cable damping", *J. Eng. Mech.*, **132**(3), 268-278. https://doi.org/10.1061/(ASCE)0733-9399(2006)132:3(268).
Duan, Y.F., Ni, Y.Q. and Ko, J.M. (2005), "State-derivative feedback control of cable vibration using semi-active MR dampers", *Comput. -Aided Civil Infrastruct. Eng.*, **20**(6), 431-449. https://doi.org/10.1111/j.1467-8667.2005.00396.x.
Duan, Y.F., Ni, Y.Q., Zhang, H.M., Spencer, Jr., B.F. and Ko, J.M. (2019a), "Design formulas for vibration control of taut cables using passive MR dampers", *Smart Struct. Syst.*, Accepted.
Duan, Y.F., Ni, Y.Q., Zhang, H.M., Spencer, Jr., B.F. and Ko J.M. (2019b), "Design formulas for vibration control of sagged cables using passive MR dampers", *Smart Struct. Syst.*, Accepted.
Duan, Y.F., Ni, Y.Q. and Ko, J.M. (2006), "Cable vibration control using magnetorheological dampers", *J. Intel. Mat. Syst. Str.*, **17** (4), 321-325.
Ehsan, F. and Scanlan R.H. (1990), "Damping stay cables with ties", *Proceedings of the 5th US-Japan Bridge Workshop*, 203-217.
Fujino, Y. and Hoang, N. (2008), "Design formulas for damping of a stay cable with a damper" *J. Struct. Eng.*, **134**(2), 269-278. https://doi.org/10.1061/(ASCE)0733-9445(2008)134:2(269).
Giaccu, G.F. and Caracoglia, L. (2012), "Effects of modeling nonlinearity in cross-ties on the dynamics of simplified in-plane cable networks", *Struct. Control Health Monit.*, **19**(3), 348-369. https://doi.org/10.1002/stc.435.
Irvine, H.M. (1981), *Cable Structures*, MIT Press, Cambridge, Massachusetts, US.
Krenk, S. (2000), "Vibration of a taut cable with an external damper", *J. Appl. Mech.*, **67**(4), 772-776. doi:10.1115/1.1322037.
Kumarasena, S., Jones, N.P. and Irwin, P. and Taylor, P. (2007), Wind-induced vibration of stay cables, FHWA-HRT-05-083, US Department of Transportation, Federal Highway Administration.
Li, H., Liu, M. and Ou, J.P. (2004), "Vibration mitigation of a stay cable with one shape memory alloy damper", *Struct. Control Health Monit.*, **11**(1), 21-36. https://doi.org/10.1002/stc.29.
Lu, L., Duan, Y.F., Spencer, B.F., Jr., Lu, X.L. and Zhou, Y. (2017), "Inertial mass damper for mitigating cable vibration", *Struct. Control Health Monit.*, e1986, https://doi.org/10.1002/stc.1986.
Or, S.W., Duan, Y.F., Ni, Y.Q., Chen, Z.H. and Lam, K.H. (2008). "Development of magnetorheological dampers with embedded piezoelectric force sensors for structural vibration control", *J. Intel. Mat. Syst. Str.*, **19**(11), 1327-1338. https://doi.org/10.1177/1045389X07085673.
Sun, L.M., Shi, C., Zhou, H.J. and Cheng, W. (2004), "A full-scale experiment on vibration mitigation of stay cable", IABSE Symposium Report, **88**(6), 31-36.
Sun, L.M., Shi, C., Zhou, H.J. and Zhou, Y.G. (2005), "Vibration mitigation of long stay cable using dampers and cross-ties", *Proceedings of the 6th International Symposium on Cable Dynamics*, Charleston, SC, USA, September.
Sun, L.M., Zhou, Y.G. and Huang, H.W. (2007), "Experiment and damping evaluation on stay cables connected by cross ties", *Proceedings of the 7th International Symposium on Cable Dynamics*. Vienna, Austria.
Virlogeux, M. (1998), "*Cable vibrations in cable-stayed bridges*", Bridge Aerodynamics, Copenhagen, Denmark.
Wang, X.Y., Ni, Y.Q., Ko, J.M. and Chen, Z.Q. (2005), "Optimal design of viscous dampers for multi-mode vibration control of bridge cables", *Eng. Struct.*, **27**(5), 792-800.

https://doi.org/10.1016/j.engstruct.2004.12.013.
Xu, Y.L., Chen, J., Ng, C.L. and Zhou, H.J. (2008), "Occurrence probability of wind-rain-induced stay cable vibration", *Adv. Struct. Eng.*, **11**(1), 53-69. https://doi.org/10.1260/136943308784069487.
Yamaguchi, H. and Nagahawatta, H.D. (1995), "Damping effects of cable cross ties in cable-stayed bridges", *J. Wind Eng. Ind. Aerod.*, **54-55**, 35-43. https://doi.org/10.1016/0167-6105(94)00027-B.
Zhou, H.J. and Sun, L.M. (2008), "Parameter optimization of damper with stiffness for stay cable", *Chinese Quarterly of Mech.*, **29**(1), 180-185. (In Chinese)
Zhou, H.J. and Sun, L.M. (2013), "Damping of stay cable with passive-on magnetorheological dampers: a full-scale test", *Int. J. Civil Eng.*, **11**(3), 154-159.
Zhou, H.J. and Xu, Y.L. (2007), "Wind-rain-induced vibration and control of stay cables in a cable-stayed bridge", *Struct. Control Health Monit.*, **14**(7), 1013-1033. https://doi.org/10.1002/stc.190.
Zhou, H.J., Huang, X.J., Xiang, N., He, J.W., Sun, L.M. and Xing, F. (2018a), "Free vibration of a taut cable with a damper and a concentrated mass", *Struct. Control Health Monit.*, **25**(11), 1-21. https://doi.org/10.1002/stc.2251.
Zhou, H.J., Qi, S.K., Yao, G.Z., Zhou, L.B., Sun, L.M. and Xing, F. (2018b), "Damping and frequency of a model cable attached with a pre-tensioned shape memory alloy wire: Experiment and analysis", *Struct. Control Health Monit.*, **25**(2), 1-19. https://doi.org/10.1002/stc.2106.
Zhou, H.J., Sun, L.M. and Shi, C. (2006), "A full-scale experimental study on cable vibration mitigation with friction damper", *J. Tongji University*, **34**(7), 864-868. (In Chinese)
Zhou, H.J., Sun, L.M. and Xing, F. (2014a), "Free vibration of taut cable with a damper and spring", *Struct. Control Health Monit.*, **21**(6), 996-1014. https://doi.org/10.1002/stc.1628.
Zhou, H.J., Sun, L.M. and Xing, F. (2014b), "Damping of full-scale stay cable with viscous damper: experiment and analysis", *Adv. Struct. Eng.*, **17**(2), 265-274. https://doi.org/10.1260/1369-4332.17.2.265.
Zhou, H.J., Xiang N., Huang X.J., Sun, L.M., Xing, F. and Zhou R. (2018c), "Full-scale test of dampers for stay cable vibration mitigation and improvement measures", *Struct. Monit. Maint.*, **5**(4), 489-506. https://doi.org/10.12989/smm.2018.5.4.489.
Zhou, H.J., Yang, X., Sun, L.M. and Xing, F. (2015), "Free vibrations of a two-cable network with near-support dampers and a cross-link", *Struct. Control Health Monit.*, **22**(9), 1173-1192. https://doi.org/10.1002/stc.1738.
Zhou, H.J., Yang, X., Zhou, R., Sun, L.M. and Xing, F. (2019), "Damping and frequency of twin cables with a crosslink and a viscous damper", *Smart Struct. Syst.*, Accepted.

Appendix

$$U_{j1} = \frac{T_j}{2}\int_0^{l_{j1}} \left(\frac{\partial Y_{j1}}{\partial x_{j1}}\right)^2 dx_{j1} = \frac{T_j A_{j1}^{\ 2}}{4L_j}\left[\frac{\pi f_j \beta}{\sin\left(\pi f_j \beta \varepsilon_j\right)}\right]^2 \times\left[\varepsilon_j + \frac{1}{2\pi f_j \beta}\sin\left(2\pi f_j \beta \varepsilon_j\right)\right] \tag{A1}$$

$$U_{j2} = \frac{T_j}{2}\int_0^{l_{j2}} \left(\frac{\partial Y_{j2}}{\partial x_{j2}}\right)^2 dx_{j2} = \frac{T_j A_{j2}^{\ 2}}{4L_j}\left\{\frac{\pi f_j \beta}{\sin\left[\pi f_j \beta\left(1-\varepsilon_j\right)\right]}\right\}^2 \times\left\{\left(1-\varepsilon_j\right) + \frac{1}{2\pi f_j \beta}\sin\left[2\pi f_j \beta\left(1-\varepsilon_j\right)\right]\right\} \tag{A2}$$

$$E_{jp} = \frac{U_{jp}}{\sum_{j=1}^{2}\sum_{p=1}^{2} U_{jp}} \tag{A3}$$